International Journal of Gender, Science and Technology
..ISSN: 2040-0748
UGC Care Group I Journal
Vol-10 Issue-02 Sep 2021

Mechanical and microstructural characterization of friction stir processed AA6061-T6 joints reinforced with nano sized particles

Pradipta Kumar Rout, Jagannath Mohapatra
Department of Mechanical Engineering, College of Engineering Bhubaneswar, Biju Patnaik University of Technology, Bhubaneswar, India

Mail ID: dash_bijay@gmail.com

Abstract

Nowadays, friction stir spot welding (FSSW) is becoming a serious candidate technology to join aircraft materials such as AA2024-O and AA6061-T6 since the use of FSSW offers significant weight savings compared to a conventional riveting technique. However, some issues, especially related to mechanical properties of FSSW joints still exist. To address these problems, the present investigation aims to study effects of tool rotation speed and pin geometry on microstructure and mechanical strength of dissimilar friction stir spot welded AA2024-O/AA6061-T6 joints. The welding processes were conducted using two different tool pins, namely cylindrical and stepped pins at varying tool rotation speeds of 900 rpm, 1400 rpm and 1800 rpm. Subsequently, experimental works including microstructural observation, microhardness measurements, lap shear tests combined with fractography analysis were conducted. Results showed that an increase in tool rotation speed resulted in microstructural coarsening in stir zone (SZ). In addition, the tool rotation speed together with the pin affected the material flow hence hook characteristics. It was found that the dissimilar friction stir spot AA2024-O/AA6061-T6 welded joint having excellent lap shear failure load (LSFL), typically 4468.4 N was produced using a cylindrical pin at the tool rotation speed of 1400 rpm. Under this lap shear testing, the mode of failure changed from shear to mixed mode failure as the tool rotation speed was increased. It seemed that hook characteristics, grain size and precipitation hardening were the key factors influencing the weld mechanical properties.

Introduction

The demand for lightweight vehicles for reducing fuel con- sumption and hence, gas emission in transportation sector such as automotive, shipbuilding, and railway industries has led to the increasing use of aluminum alloys. The alloys are light metals which have several advantages such as high

strength to weight ratio, extremely good sound damping capability, excellent damage tolerance and good corrosion resistance [1,2]. Among these alloys, aluminum 2000 series (AleCu) and aluminum 6000 series (AleMgeSi) are the most commonly used materials in aircraft and automotive industries [3]. Both alloys are categorized as high- strength aluminum alloys with their strengths are increased by precipitation hardening but in term of weldability, 6000 alloys are readily welded using conventional fusion welding techniques whereas 2000 alloys are less weldable [4]. A significant advance has been made in welding technology marked by the invention of friction stir welding (FSW) in 1991 which enables unweldable aluminum 2000 and 7000 series to be joined without solidification cracking since FSW process is carried out without melting. Furthermore, a new variant of FSW known as friction stir spot welding (FSSW) was introduced by Mazda Motor Corporation and Kawasaki Heavy Industries in 2003 [5e7]. This FSSW technique is especially used for joining sheet metals and structural parts in automotive industry.

The use of lightweight metals, for example, aluminum alloys to replace steels in the fabrication of vehicle structures has created a challenge. This is because resistance spot welding (RSW) which has been the main welding technique for joining steel sheets or steel components in the vehicle industry is not suitable for joining aluminum alloys due to some disadvantages such as high current requirement owing to their high thermal conductivity, metallur- gical defects in the weld nugget zone which lead to poor me- chanical performance and lack of consistency in the weld quality [8e10]. Therefore, an innovative joining technology such as FSSW is becoming a promising alternative for joining aluminum and it has a potency to replace RSW in the future.

During the last few years, numerous efforts have been made to improve mechanical properties of FSSW joints by analyzing process parameters including pin, tool rotation speed, plunge depth of shoulder and dwell time. It has been reported that the tools having shorter pin and high total penetration depth increased cross ten- sion and lap shear loads due to increased effective bonding length [11]. Subsequently, Piccini and Svoboda [12] have shown that the pin influenced the quality of FSSW joints. According to the re- searchers, a half-threaded pin was excellent to produce large bonding width resulting in higher cross tension failure load. Another report showed

that a threaded pin could also maximize the tensile shear failure load of FSSW joints [13]. Recently, Garg and Bhattacharya [14] have conducted comparative study of circular tool pin and square tool pin with the results showed that the former produced more heat, whereas the later generated more strain owing to plastic deformation in the base metal caused by the tool pin corners. As a result, the square tool pin was more beneficial since it produced FSSW joints with improved strength.

Apart from the pin, tool rotation speed is also the key factor affecting the quality of FSSW joints. Some researchers [15e17] have shown that an increase in tool rotation speed improved the tensile shear load. These improved mechanical properties under high tool rotation speed were associated with weld microstructure and changes in the hook geometry, i.e., increased hook width and low hook height [18e20].

In modern structural applications, welding of dissimilar metals sometimes has to be done for optimization of properties such as weight, mechanical strength, toughness and corrosion. It is also applied at the situation where the use of more expensive single metal only is restricted due to economic reasons [21]. However, the welding of dissimilar metal using conventional fusion welding is particularly difficult due to differences in physical, chemical, metallurgical and thermomechanical properties [22,23]. Therefore, solid state welding processes such as FSW and its variant such as FSSW have become candidate technology to join the different materials. Numerous works on FSSW have been conducted to join dissimilar metals between aluminum alloys to other metals including steels [24e26], copper [27e29] and magnesium [30e32]. In addition, advances have also been made in FSSW of aluminum series which involve non heat treated 5000 aluminum alloys and heat treated aluminum 2000, 6000, and 7000 series. Among these aluminum alloys, high-strength AA2024-T3 and AA6061-T6 aluminum alloys are widely used in lightweight vehicles or struc- tures and welding of these dissimilar alloys is critical, especially when it is required to produce high quality welds. In recent years, there have been few studies on dissimilar FSSW of particular aluminum alloys such as AA2024-T3 and AA6061-T6. Ibrahim and Yapici [33] have endeavored to improve the performance of dis- similar FSSW 2024-T3/6061-T6 weld joint by introducing inter- mediate layer to remove keyhole. The results showed that the additional material

caused the hook formation to extend into upper sheet resulting in a weld nugget zone with improved strength. Subsequently, attempts have been made by Paidar et al. [34] to join AA2024-T3/AA6061-T6 dissimilar metals using a modified FSSW known as the modified friction stir clinched (MFSC) with specific attentions are paid to materials positioning. According to the au- thors, microstructure, hardness distribution and fracture morphology were strongly influenced by flow behavior material induced by sheet position and better weld tensile strength, typi- cally 97.88 MPa was produced using AA2024-T3/AA6061-T6 posi- tion than AA6061-T6/AA2024-T3 position.

Despite several works on dissimilar friction stir spot 2024-T3/6061-T6 weld joints have been reported, it seems that data related to the effects of pin geometry, especially for a stepped pin and tool rotation speed on microstructure and mechanical properties of such weld joints are limited. Therefore, further detailed investiga- tion needs to be carried out. In this study, AA2024-O and AA6061- T6 sheets were joined using FSSW with AA2024-O was located as the upper sheet. FSSW processes were conducted at various tool rotation speeds using two types of tool pin, i.e., cylindrical pin and step pin. Furthermore, the weld mechanical properties under different weld parameters were discussed.

2. Materials and methods

2.1 Materials and tooling

In this study, materials used to produce friction stir spot welded lap joints were 3-mm thick AA2024-O and AA6061-T6 aluminum alloy sheets and their chemical compositions. Two types of tool pins, namely cylindrical pin and stepped pin were used with their dimensions are shown in Fig. 1. The cylindrical pin had a pin diameter of 5 mm and a pin height of 5 mm, whereas the stepped pin had three different steps having the diameters of 8 mm (1st step), 6 mm (2nd step) and 4 mm (3rd step) with the total height of the pin was 5 mm similar to that of the cylindrical pin. The pin diameter of the cylindrical pin was made in between the 1st step and 3rd step diameters of the stepped pin so that the friction heat generated by both pins was not significantly different. The FSSW tools were made of AISI H13 tool steel which had been hardened by oil quenching to obtain the required hardness, typi- cally around 58 HRC.

2.2 Friction stir spot welding

FSSW process was conducted using a vertical universal milling machine to

produce lap welded sheets with AA2024-O and AA6061-T6 were positioned as upper and lower sheets respectively as shown in Fig. 2. The welding processes were carried out at varying tool rotation speeds of 900, 1400 and 1800 rpm. Other processing parameters including dwell time and shoulder plunge depth were maintained constant, typically of 5 s and 0.1 mm respectively. The thermal cycles during welding were recorded

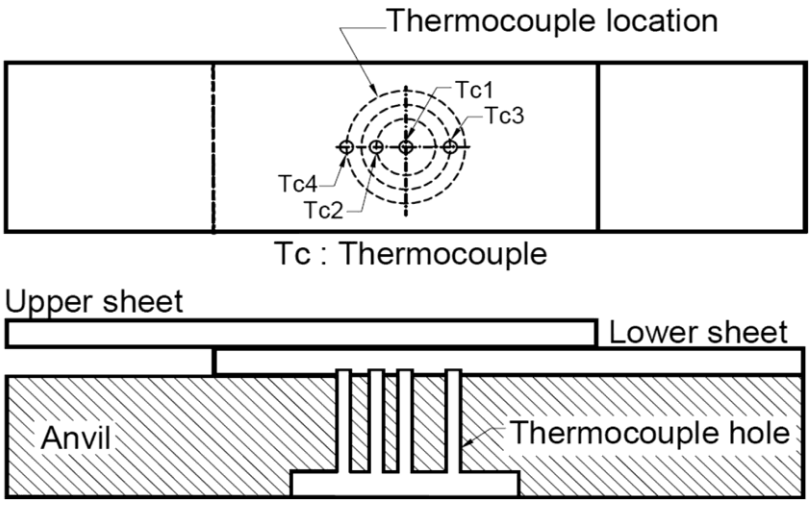

Fig 1 Types of tools used

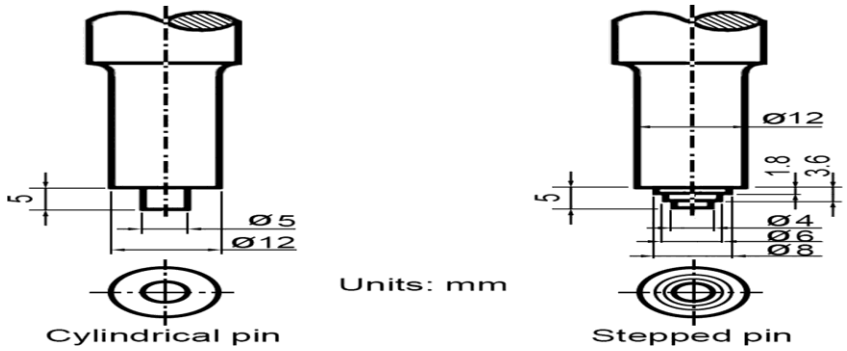

Fig. 2 Schematic of clamping system showing the locations of holes at which the thermocouples were inserted.

using K-type thermocouples, namely Tc1, Tc2, Tc3 and Tc4 inserted into the holes at the bottom part of the lower sheet. The locations of thermocouple were

determined at the distances of 0, 4, 6 and 8 from the weld center respectively. Macro- and microstructure observations were conducted using optical microscopy on the cross section of the friction stir spot welded lap joints. Various microstructure zones in the weld joints were characterized. For this reason, standard metallographic technique was applied for sample preparation and the etchant used was Keller's reagent containing 2 mL HF, 3 mL HCl, 5 mL HNO_3 and 190 mL H_2O.

2.4 Microhardness measurements

The measurements of Vickers microhardness (HV) were carried out on the cross section of the lap joints along both upper sheet and lower sheet as shown in Fig. 3. The measurement lines were located at three different regions, i.e., (a) the upper sheet at the distance of 1 mm from the contacting sheet surfaces, (b) the lower sheet with the position of measurement line is symmetrical to that of the upper sheet and (c) the region underneath the keyhole. The center to center distance of measurement was 500 mm whereas the load and dwell time used in this study were 100 gf and 10 s respectively.

3.Results and discussion

3.1 Weld thermal cycles

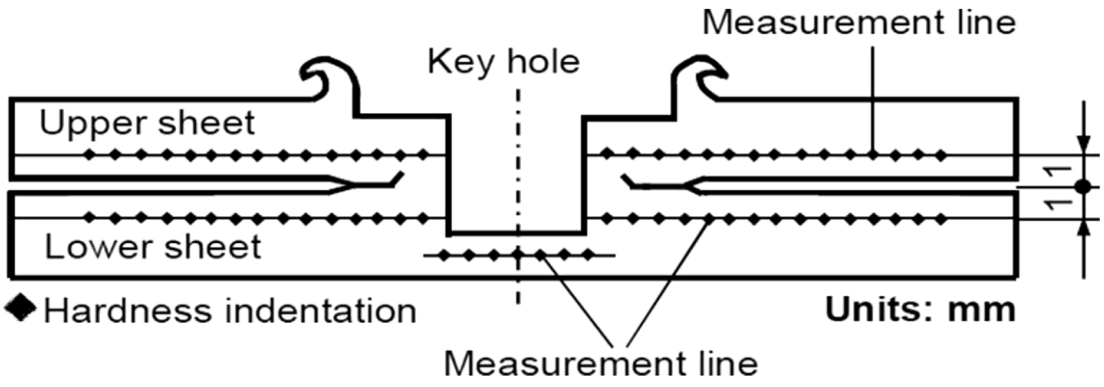

Fig. 3. Locations of microhardness measurements along: upper sheet, lower sheet and the region underneath a keyhole at the bottom of lower sheet surface.

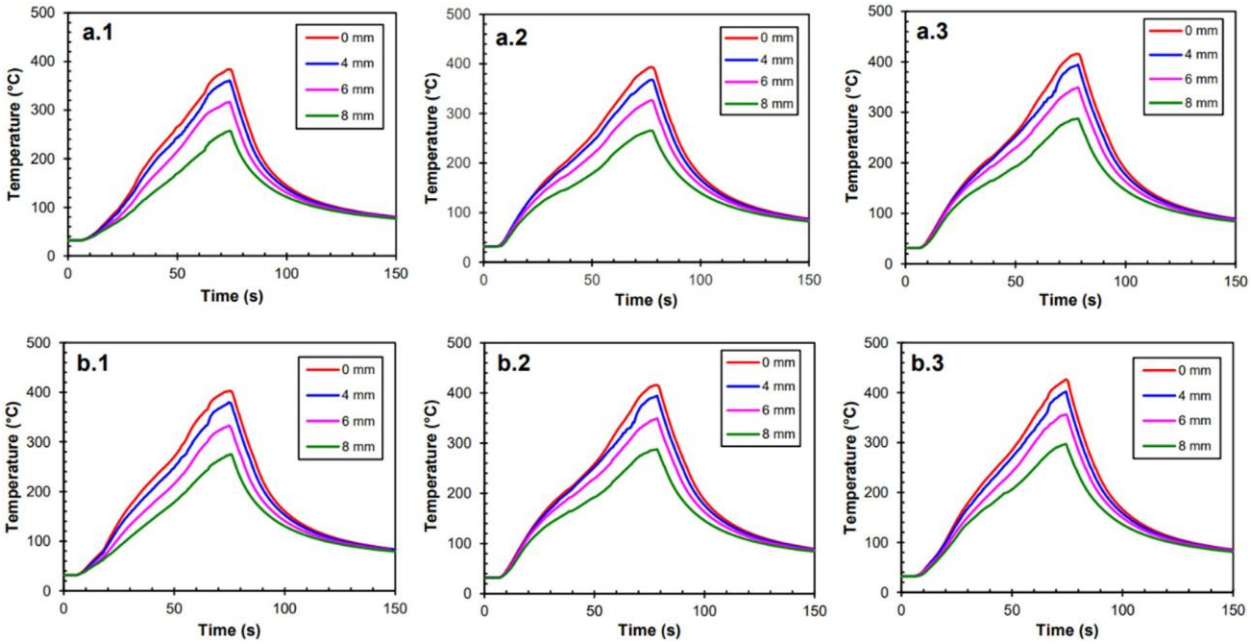

Fig. 5. Weld thermal cycles obtained at the distance of 0, 4, 6 and 8 mm from the weld center. Note: (a) and (b) represent cylindrical and stepped pins respectively and (1), (2), and (3) represent tool rotation speeds of 900, 1400 and 1800 rpm, respectively.

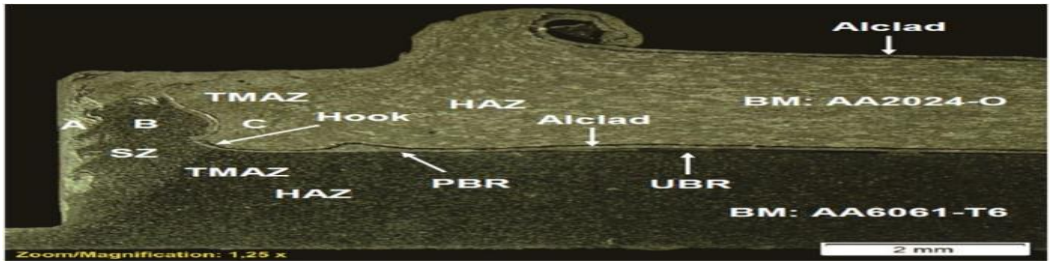

Fig. 6. Cross-sectional appearance of FSS welded dissimilar AA2024-O/AA6061-T6 joint produced using a cylindrical pin at 900 rpm.

3.2Macro- and microstructural examinations

3.2.1 Microstructures of the welds

Fig. 6 shows an example of weld macrostructure in dissimilar friction stir spot welding of AA2024-O/AA6061-T6 sheets using a cylindrical pin at a tool rotation speed of 1400 rpm. Of note is that since AA2024-O and AA6061-T6 have different etching response to Keller's reagent so that the material flow of the two alloys can be clearly distinguished where the dark-etched regions in Fig. 6 are 6061-T6 material and in contrast, the AA2024-O appears bright. Referring to Fig. 6, it can be seen that the weld joint consists of various distinct microstructural regions, namely stir zone (SZ), thermomechanically affected zone (TMAZ), heat affected zone (HAZ), partially bonded region (PBR) and

unbonded region (UBR). The macrograph also reveals the presence hook which is the interface between upper and lower sheets near SZ and it is bent upward towards upper sheet due to combined effect of plunging and stirring during welding [18]. Another feature observed in Fig. 6 is the presence of thin layers with its thickness around 200 mm at the AA2024-O sheet surfaces known as Alclad. Of note is that in aerospace industry, Alclad layer is commonly used to improve the corrosion resistance of high strength AA2024 aluminum alloy [38]. The energy dispersive X-ray (EDX) spectra taken from some distinct regions in Fig. 6 are shown in Fig. 7. It can be seen that the region near the keyhole surface marked A in Fig. 6 shows the presence of high alloying elements, typically 3.95 wt% Cu and 1.34 wt % Mg with the significant amount of O as shown in Fig. 7a. This Cu and Mg-rich layer probably comes from AA2024-O material underneath the shoulder which moves downward as the tool is plunged into the sheets. Subsequently, the region marked B in SZ (Fig. 6) consists of 1.81 wt% Cu with the amount of Mg around 0.77 wt% as shown in Fig. 7b. It seems that this chemical compo- sition is a result of an intermixing between AA2024-O and AA6061- T6 materials during welding. The bright etched region adjacent to SZ marked C in Fig. 6 contains 3.00 wt% Cu as the main alloying element as shown in Fig. 7c reflecting the bulk chemical compo- sition of AA2024-O. On the other hand, EDX-spectra taken from Alclad layer reveals Al as the only element as shown in Fig. 7d whereas the peak of oxygen is not considered as the alloying element.

The photomicrographs taken from various microstructural zones in Fig. 6 are shown in Fig. 8. The microstructure of AA6061-T6 base metal (lower sheet) in Fig. 8a.1 consists of elongated grains which are parallel to the rolling direction. Fig. 8a.1 also reveals the presence of dispersed dark coarse intermetallic particles which precipitate within the grains and along the grain boundaries. Ac- cording to some researchers [39,40], these second phase particles seem to be b (Mg_2Si) which commonly form in the 6000 series under T6 treatment. Such

elongated grains are also observed in the weld.

3.2.2 Effect of pin and rotation speed

Results of microstructural examinations taken from SZ of the dissimilar metal friction stir spot welds are shown in Fig. 9. The SZ microstructures for all weld joints under study are composed of mainly fine equiaxed or polygonal grains as a result of dynamic recrystallization during welding. In addition, the results confirm that increasing tool rotation speed increases the grain size. It has been reported that the formation of coarse grains is associated with high friction heat which causes grain growth [44]. Another finding in this investigation is that in comparison with the cylindrical pin, the weld joints produced using the stepped pin have coarser mi- crostructures. These results seem to be consistent with the weld.

3.2.3 Material flow characteristics

Fig. 10 shows cross sections of dissimilar FSSW joints between AA2024-O and AA6061-T6 produced using two different tool pin geometries, namely cylindrical and stepped pins at varying tool rotation speeds of 900, 1400 and 1800 rpm. It can be seen that various regions in all weld joints can be clearly distinguished therefore, the trace of material flow during welding may be easily studied. Referring to Fig. 10, it can be seen that as the tool rotation speed increases, the degree of extrusion of AA6061-T6 lower sheet material (appears dark) into AA2024-O upper sheet (bright region) rises for both cylindrical and stepped pins but the bond width tends to decrease. In addition, the FSSW joints produced using the stepped pin have lower extrusion into the upper sheet compared to the cylindrical pin. It seems that during FSSW process, the upward- directed material flow in the stepped pin is retarded once the material flow from the lower pin comes into contact with the horizontal plane (shoulder) of the larger pin above it.

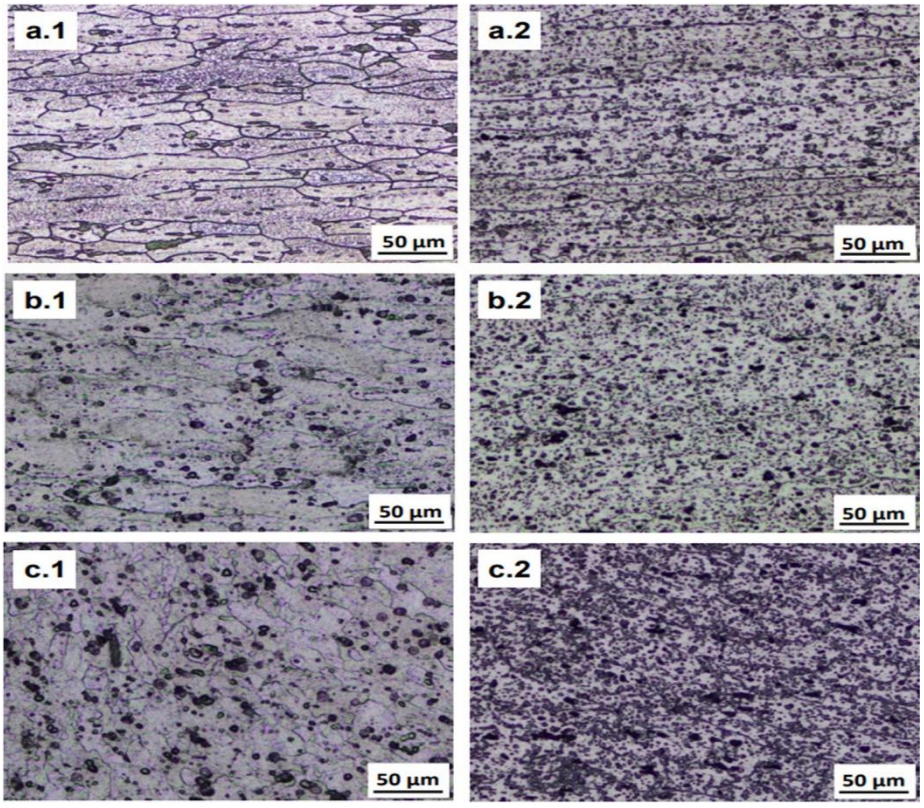

Fig. 8. Typical microstructures present at: (a), (b) and (c) base metal, HAZ and TMAZ respectively for: (1) AA6061-T6 lower sheet and (2) AA2024-O upper sheet in Fig. 6.

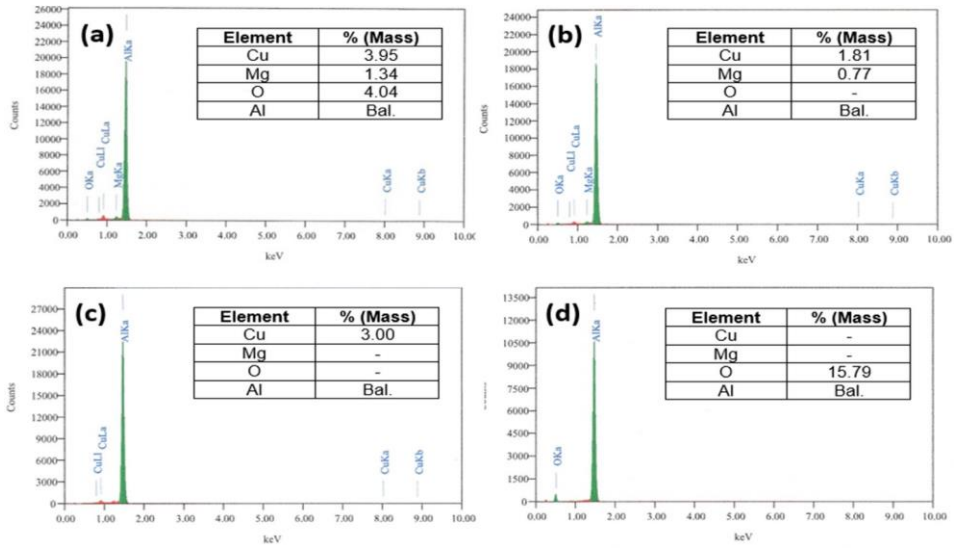

Fig. 7. EDX-spectra of the regions marked: (a) A, (b) B, (c) C and (d) Alclad in Fig. 6.

flow is deflected in the outward direction resulting in shallow penetration into AA2024-O upper sheet.

Based on previous reports [5,46,47], material flow characteris- tics in a cylindrical pin are proposed as shown in Fig. 11a. As the rotating tool plunges into the lapped sheets and its shoulder comes into contact with the AA2024-O upper sheet surface then the ma- terials around the pin flow in three directions. First, the materials beneath the shoulder flow inward towards the pin root as indicated by (1) in Fig. 11a. Secondly, the materials are pushed downward towards the pin bottom (2) and finally, the adjoining lower sheet materials, namely AA6061-T6 adjacent the pin bottom flow upward and extrude into the upper sheet (3). As a result, intermixing be- tween the two sheet materials occurs resulting in stir zone (SZ) accompanied by upward hooking formation. The three material flow directions in the cylindrical pin in Fig. 11a are likely to occur in each pin step of the stepped pin. If this mechanism is operative then the material flow characteristics for the stepped pin is proposed as shown in Fig. 11b. In this condition, the material flow in the upward direction is retarded once it comes into contact with the shoulder of larger pin hence reducing the material extrusion towards the upper sheet. It seems that changes in the material flow under different tool pin and tool rotation speed affect the hook geometry.

Further microstructural examinations on the hook dimensions given in bond width and bond height for all welds under study are shown in Fig. 12. It can be seen that the bond width of the weld produced by cylindrical pin at 900 rpm is around 1.567 mm. As the tool rotation speed is increased to 1400 rpm, the bonding width slightly reduces to 1.419 mm. However, more increase in the tool rotation speed up to 1800 rpm reduces the bond width to

1.260 mm. Unlike bond width, the hook height of these weld joints increases with increasing tool rotation speed. It seems likely that changes in hook geometry is associated with the material flow in the upward direction and as a consequence, the interface between upper and lower sheets (hook) is severely bent upward at a higher tool rotation speed hence resulting in increased hook height.

In comparison with the cylindrical pin, the hook geometry resulted from the stepped pin are characterized by larger bond width but shorter hook height. These results could be linked to retardation of upward-directed material flow by shoulders of different pins so that the materials underneath the pins are forced to flow outward. However, at a high tool rotation speed, i.e. 1800 rpm, the stirring forces are sufficient to push the materials underneath the stepped pins to flow in the outward and also up- ward directions. In such a condition, the bond width of the stepped pin is larger with lower hook height compared to those resulted from the cylindrical pin at the same tool rotation speed.

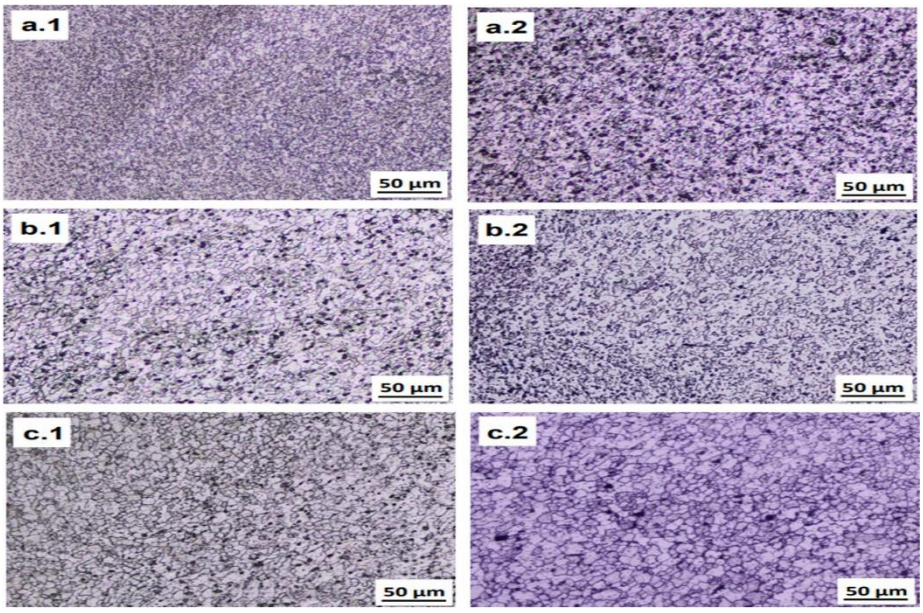

Fig. 9. Variation in stir zone (SZ) microstructures at tool rotation speeds of: (a), (b) and (c) 900, 1400 and 1800 rpm respectively produced using: (1) cylindrical and (2) stepped pin.

3.3 Mechanical properties

3.3.1 Hardness profiles

Fig. 13 shows hardness distributions taken from the cross sec- tions of the dissimilar friction stir spot welded AA2024-O/AA6061- T6 sheets produced using two different tool pins at varying tool rotation speeds. It is seen that the hardness distributions for all weld joints under study are symmetrical about the weld center. The average hardness of AA2024-O upper sheet is around 57.3 HV whereas the AA6061-T6 lower sheet has a relatively higher hard- ness, typically 76.8 HV. For each weld joint in Fig. 13, the hardness of AA2024-O upper sheet increases exponentially as the distance moves from the base metal towards HAZ and TMAZ until a maximum value of hardness is achieved. After this point, a sharp drop in the hardness is observed in stir zone (SZ). Furthermore, a peak of hardness re-appears at the region close to keyhole surface which is composed of mainly AA2024-O. It seems likely that the high values of hardness in HAZ and TMAZ of AA2024-O upper sheet are related to precipitation hardening whereas in the keyhole surface, the peak of hardness is attributed to combined effect of precipitation hardening and work hardening. On the other hand, the decrease of hardness in SZ is associated with the reduction in dislocation density as a result of dynamic recrystallization during welding. Unlike AA2024-O upper sheet, the AA6061-T6 lower sheet decreases steadily as the distance approaches the keyhole surface. This softening in the AA6061-T6 lower sheet including HAZ and TMAZ is associated with annealing effect during welding which causes coarsening or even dissolution of strengthening b (Mg_2Si) precipitates which leads to over aging [48]. The hardness distri- bution along the region underneath the keyhole in the AA6061-T6 lower sheet is marked by the presence of a peak of hardness at the weld center and then the hardness decreases continuously towards the keyhole surface hence forming normal distribution-like curve. Effects of tool rotation speed on the hardness seen this inves- tigation are summarized as follows. The hardness values across HAZ, TMAZ and SZ of AA2024-O upper sheet increase as the tool rotation speed is increased for both cylindrical and stepped pins. In contrast, the

hardness of AA6061-T6 lower sheet slightly decreases with lowering tool rotation speed whereas the peak of hardness in the region underneath the keyhole tends to decrease especially for stepped pin. These results seem to suggest that high friction heat due to increased tool rotation speed causes softening in AA6061-T6 lower sheet as a result of coarsening and dissolution of precipitates.

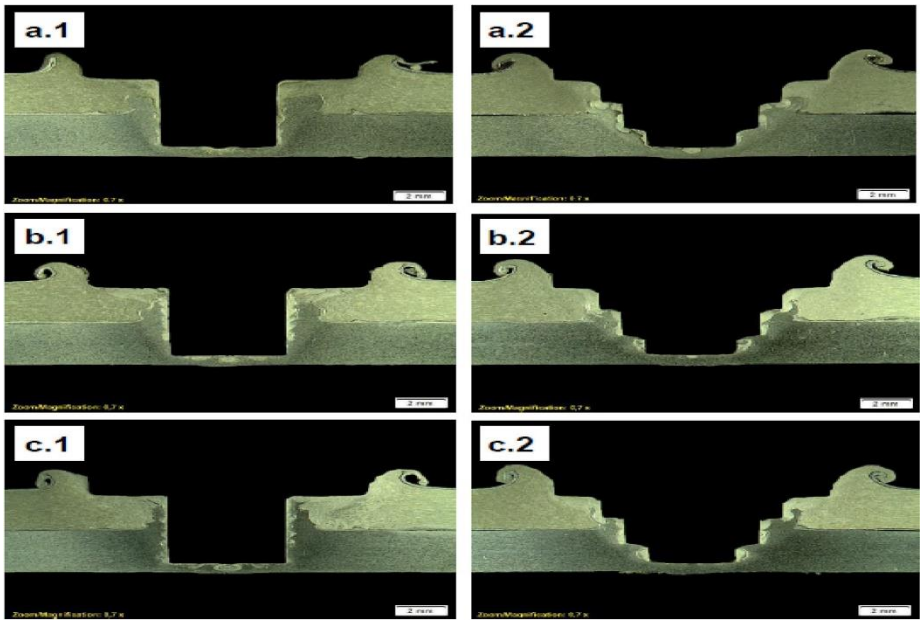

Fig. 10. Cross-sectional macrographs of dissimilar AA2024-O/AA6061-T6 weld joints prepared using: (1) cylindrical pin and (2) stepped pin at tool rotation speeds of: (a), (b) and (c) 900, 1400 and 1800 rpm respectively.

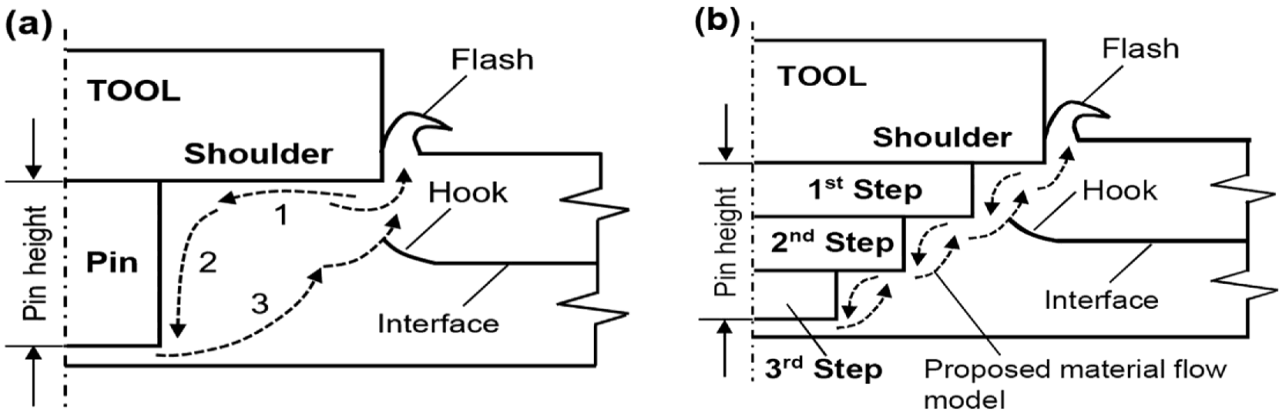

Fig. 11. Material flow characteristics in: (a) cylindrical pin and (b) stepped pin.

Apart from the tool rotation speed, pin geometry plays a sig- nificant role in determining the hardness distribution. As seen previously, the SZ of the weld produced using the cylindrical pin has relatively high hardness compared to that produced using the stepped pin. In addition, the pin geometry also influences the hardness profiles along the region underneath the keyhole. In this region, the high values of hardness for the cylindrical pin are observed in the weld center and its adjacent area so that the width of high hardness regions is relatively large. In contrast, the high hardness region in the stepped pin is concentrated at the weld. center only hence forming narrow high hardness region. These results could be linked to the difference in the pin diameter in which the higher pin diameter as seen in the cylindrical pin pro- vides larger friction area and work hardening resulting in high hardness in the regions around the weld center.

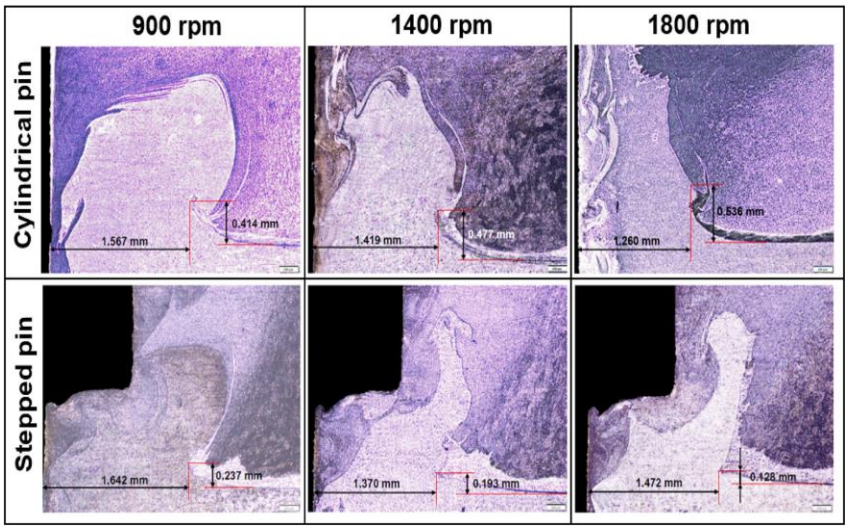

Fig. 12. Variations in hook geometry and size under different tool pins and tool rotation speeds.

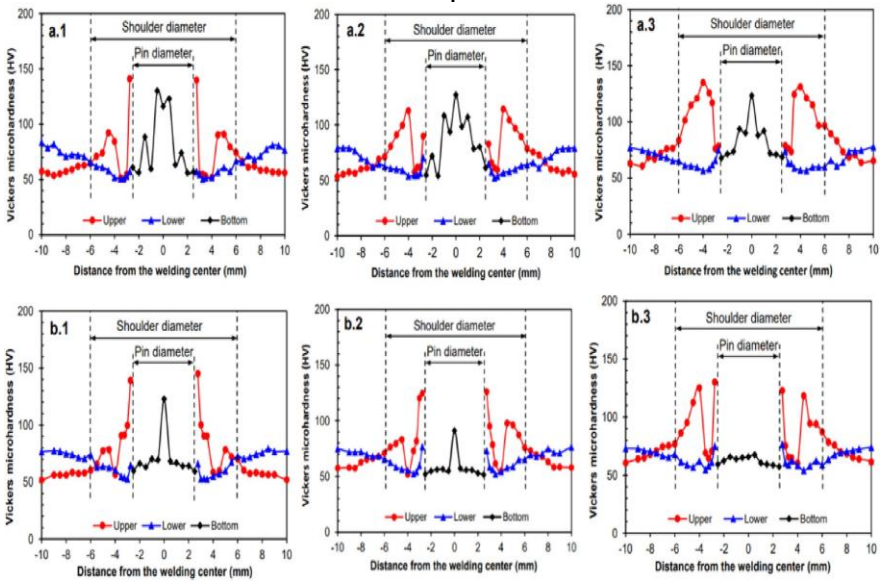

Fig. 13. Microhardness distributions across the weld joints resulted from: (a) and (b) tool pin and stepped pin respectively at tool rotation speeds of: (1), (2) and (3) 900, 1400 and 1800 rpm respectively

3.3.2 Lap shear failure load properties

Fig. 14 shows the results of lap shear tests of the welds produced using cylindrical and stepped pins at varying tool rotation speeds. It can be seen that for the cylindrical pin, increasing tool rotation speed up to 1400 rpm increases the lap shear failure load (LSFL) until a maximum value of LSFL, typically 4468.4 N is achieved. Furthermore, a considerable decrease in lap shear load occurs at a high tool rotation speed, typically 1800 rpm consistent with the previous reports [8]. A similar trend is also observed in the welds produced using the stepped pin with its LSFL values are slightly lower than the cylindrical pin at the rotation speeds of 900 and 1400 rpm. However, at the tool rotation speed of 1800 rpm, the weld produced by means of the stepped pin shows better LSFL compared to the cylindrical pin but its value is still lower than the LSFL value of the weld produced by the cylindrical pin at 1400 rpm. This finding seems to suggest that the cylindrical pin profile is more desirable compared to the stepped pin profile and the best tool rotation speed

for the cylindrical pin is attained at 1400 rpm.

The fracture surfaces taken from the upper and lower sheets for cylindrical pin at varying tool rotation speeds are shown in Fig.15. It can be seen that under the tension shear loading, the cylindrical pin reveals two fracture modes. At a low tool rotation speed, typically 900 rpm, the fracture mode is shear fracture which seems to initiate at the hook tip due to its high stress concentration. The crack then propagates across the recrystallized zone or SZ and parallel to the direction of applied load resulting in separation of the two sheets. However, as the tool rotation speeds is increased to 1400 or 1800 rpm, the fracture surface reveals mixed mode, i.e. tension- shear fracture. In such a condition, the crack which initially prop- agates in the horizontal direction deviates upward after it reaches SZ due to resistance of SZ. According to Pathak et al. [49], the crack retardation in SZ is associated with its high hardness. As a result, the load component perpendicular to the applied load direction exists resulting in an inclined crack.Fig. 16 shows fractographs of the weld joints prepared using stepped pin after lap shear tests. The fracture surface of the weld prepared at 900 rpm reveals shear fracture. It seems that the crack starts to nucleate at the hook tip and propagates parallel to the applied load direction across the hole left by the 2nd step of step- ped pin. At a higher tool rotation speed, i.e. 1400 or 1800 rpm the mode of failure changes to mixed mode as indicated by the pres- ence of inclined crack towards the corner between 1st step (largest diameter) and 2nd step in the stepped pin which has a high stress.

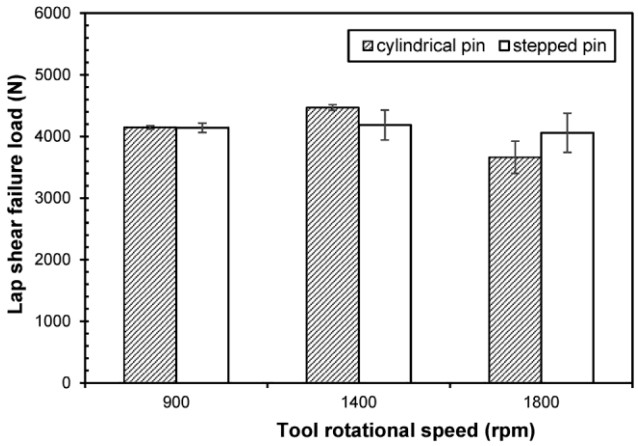

Fig. 14. Lap shear failure loads of the dissimilar metal FSSW joints under investigation

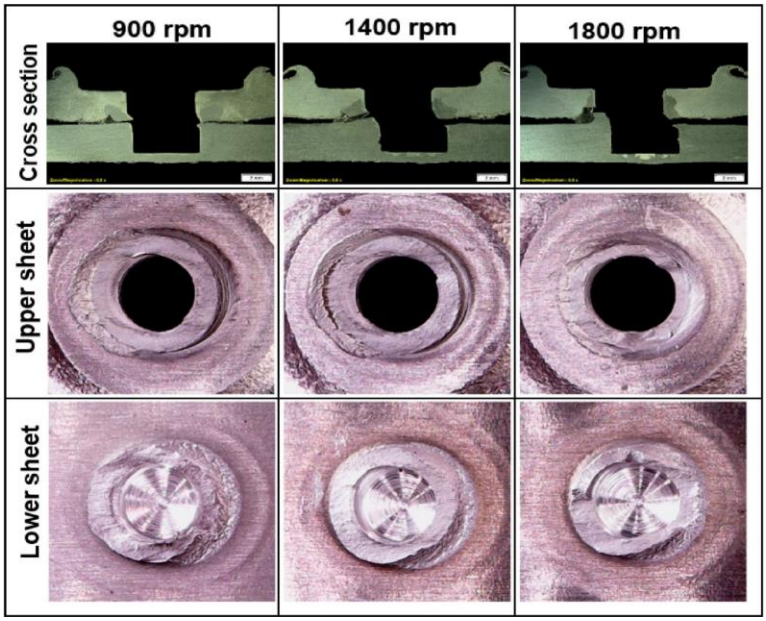

Fig. 15. Fracture surfaces of the welds produced using cylindrical pin after lap shear testing.

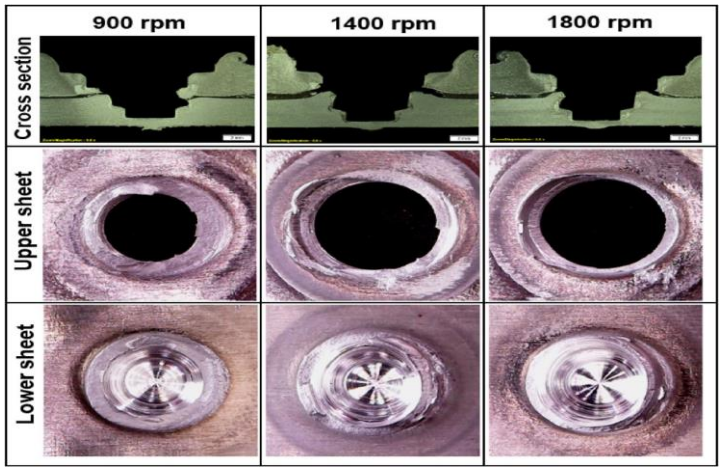

Fig. 16. Fracture surfaces of the welds produced using stepped pin after lap shear testing.

concentration. In this condition, the crack passage terminates at the 1st step leaving a larger hole at the fracture surface of the upper sheet compared to that observed in the weld at 900 rpm.

Apart from a low magnification optical microscopy, fractography studies were also conducted using scanning electron microscopy (SEM). For this purpose, the weld produced using a cylindrical pin at 1400 rpm was selected since it shows better strength and the results are given in Fig. 17. The SEM macrograph of the fracture surface is shown in Fig. 17a whereas the magnified views of the regions marked A, B and C in Fig. 17a are shown in Fig. 17bed respectively. It can be seen that the outer region of the fracture surface marked A shows the presence of scratch marks indicating shear of surfaces. Similar appearance is also observed in the inner region of the fracture surface (region D). However, the mixed failure is observed in the mid thickness of the fracture surface as indicated by the presence of several shallow dimples in matrix scratch- marked region.It seems that the shear strength of the welds under study is complex involving many factors including hook characteristics (hook height and fully bonded region) resulted from metal flow

around the pin, grain size in SZ and precipitation hardening. The results obtained from this investigation are summarized as fol- lows. As the tool rotation speed increases, the grain size in SZ increases due to high frictional heat but this undesirable effect from the view point of strength is compensated by the occurrence of precipitation hardening which improves hardness and strength of the weld joint. On the other hand, increasing tool rotation speed changes the hook geometries as indicated by increased hook height. It seems that combined effect of these parameters achieves an optimum condition at the tool rotation speed of 1400 rpm with the strengthening mechanism is governed by mainly precipitation hardening. As a comparison, Guishen et al. [50] who performed optimization study on mechanical performance of similar swept friction stir spot welding (SFSSW) of thin AA6061-T6 sheets sug- gested that

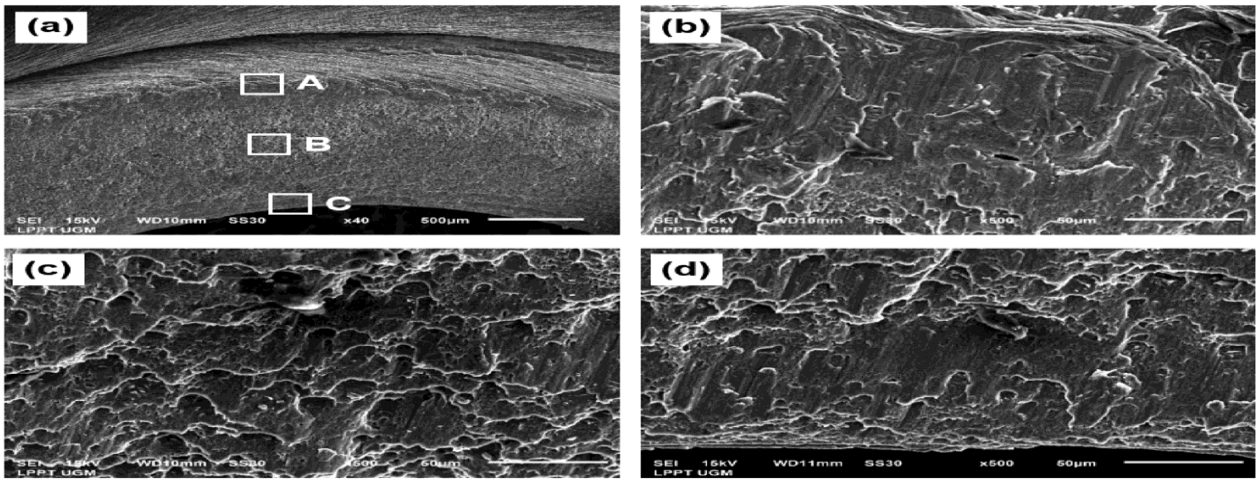

Fig. 17. (a) SEM fractograph of the weld produced using a cylindrical pin at 1400 rpm after lap shear testing and (b), (c) and (d) the magnified views outlined by A, B and C squares in Fig. 17(a) respectively

4. Conclusions

The present work has endeavored to study microstructure and mechanical properties of dissimilar metal FSSW joints between AA2024 and 6061-T6 due to effects of pin geometry and tool rotation speed and the following conclusions are drawn:Pin affects material flow characteristics which in turn hook geometry and the size of SZ. In this work, a tool having a cylindrical pin is desirable since it allows the lower sheet material around the pin to flow upward during welding without any retardation in contrast to a stepped pin resulting in better SZ.

(1) An increase in tool rotation speed increases friction heat leading to grain coarsening in SZ due to grain growth during welding.

(2) The hardness values of HAZ, TMAZ and SZ in AA2024-O up- per sheet are higher than their base metal due to precipita- tion hardening during welding and in contrast, AA6061-T6 lower sheet is suffered from softening in the weld region and its adjacent area.

(3) At a low tool rotation speed, typically 900 rpm, the weld reveals shear failure under lap shear loading for both cylin- drical and stepped pins. As the tool rotation speed is increased to 1400 or 1800 rpm, the mode of failure changes to mixed mode.

(4) The best tool rotation speed is attained at the tool rotation speed of 1400 rpm owing to a proper combination of various factors including grain size,

hook width and precipitation hardening.

Conflicts of interest

The authors declare that there is no conflicts of interest

References

[1] S. Dourandish, S.M. Mousavizade, H.R. Ezatpour, G.R. Ebrahimi, Microstruc- ture, mechanical properties and failure behaviour of protrusion friction stir spot welded 2024 aluminium alloy sheets, Sci. Technol. Weld. Join. 23 (4) (2018) 295e307.

[2] J. Shen, S.B.M. Lage, U.F.H. Suhuddin, C. Bolfarini, J.F.D. Santos, Texture development and material flow behavior during refill friction stir spot welding of AlMgSc, Metall. Mater. Trans. A 49A (2018) 241e254.

[3] C. Rajendran, K. Srinivasan, V. Balasubramanian, H. Balaji, P. Selvaraj, Feasi- bility study of FSW, LBW and TIG joining process to fabricate light combat aircraft structure, Int. J. Lightweight Mater. Manuf. 4 (2021) 480e490.

[4] G. Mathers, The Welding of Aluminium and Its Alloys, Woodhead Publishing Limited, Cambridge, 2011.

[5] R.S. Mishra, P.S. De, N. Kumar, Friction Stir Welding and Processing: Science and Engineering, Springer International Publishing, Switzerland, 2014.

[6] G.G. Yapici, I.J. Ibrahim, On the fatigue and fracture behavior of keyhole-free friction stir spot welded joints in an aluminum alloy, J. Mater. Res. Technol. 11 (2021) 40e49.

[7] Y. Bozkurt, S. Salman, G. Cam, Effect of welding parameters on lap shear tensile properties of dissimilar friction stir spot welded AA 5754-H22/2024-T3 joints, Sci. Technol. Weld. Join. 18 (4) (2013) 337e345.

[8] S. Bozzi, A.L. Helbert-Etter, T. Baudin, V. Klosek, J.G. Kerbiguet, B. Criqui, In- fluence of FSSW parameters on fracture mechanisms of 5182 aluminium welds, J. Mater. Process. Technol. 210 (2010) 1429e1435.

[9] B. Zhang, X. Chen, K. Pan, C. Yang, J-integral based correlation evaluation between microstructure

and mechanical strength for FSSW joints made of automotive aluminum alloys, J. Manuf. Process. 44 (2019) 62e71.

[10] D. Klobcar, J. Tusek, A. Smolej, S. Simoncic, Parametric study of FSSW of aluminium alloy 5754 using a pinless tool, Weld. World 59 (2015) 269e281.

[11] J.M. Piccini, H.G. Svoboda, Effect of pin length on friction stir spot welding (FSSW) of dissimilar aluminum-steel joints, Procedia Mater. Sci. 9 (2015) 504e513.

[12] Z. Li, Y. Yue, S. Ji, C. Peng, L. Wang, Optimal design of thread geometry and its performance in friction stir spot welding, Mater. Des. 94 (2016) 368e376.

[13] L. Zhou, R.X. Zhang, G.H. Li, W.L. Zhou, Y.X. Huang, X.G. Song, Effect of pin profile on microstructure and mechanical properties of friction stir spot welded Al-Cu dissimilar metals, J. Manuf. Process. 36 (2018) 1e9.

[14] A. Garg, A. Bhattacharya, On lap shear strength of friction stir spot welded AA6061 alloy, J. Manuf. Process. 26 (2017) 203e215.

[15] R.S. Shekhawat, V.N. Nadakuduru, K.B. Nagumothu, Microstructures and mechanical properties of friction stir spot welded Al 6061 alloy lap joint welded in air and water, Mater. Today: Proc. 41 (2021) 995e1000.

[16] M. Paidar, A. Khodabandeh, H. Najafi, A.S. Rouh-aghdam, Effects of the tool rotational speed and shoulder penetration depth on mechanical properties and failure modes of friction stir spot welds of aluminum 2024-T3 sheets,
J. Mech. Sci. Technol. 28 (12) (2014) 4893e4898.

[17] Z. Shen, X. Yang, Z. Zhang, L. Cui, Y. Yin, Mechanical properties and failure mechanisms of friction stir spot welds of AA 6061-T4 sheets, Mater. Des. 49 (2013) 181e191.

[18] S. Babu, V.S. Sankar, G.D.J. Ram, P.V. Venkitakishnan, G.M. Reddy, K.P. Rao, Microstructures and mechanical properties of friction stir spot welded

aluminum alloy AA2014, J. Mater. Eng. Perform. 22 (1) (2013) 71e84.

[19] P.K. Rana, R.G. Narayanan, S.V. Kailas, Effect of rotational speed on friction stir spot welding of AA5052-H32/HDPE/AA5052-H32 sandwich sheets, J. Mater. Process. Technol. 252 (2018) 511e523.

[20] Tiwan, M.N. Ilman, Kusmono, Effect of pin and tool rotational speed on microstructure and mechanical properties of friction stir spot welded joints in AA2024-O aluminum alloy, Int. J. Eng. Trans. B: Appl. 34 (8) (2021) 184e191.

[21] J.F. Guo, H.C. Chen, C.N. Sun, G. Bi, Z. Sun, J. Wei, Friction stir welding of dissimilar materials between AA6061 and AA7075 Al alloys effects of process parameters, Mater. Des. 56 (2014) 185e192.

[22] G. Sorger, H. Wang, P. Vilaca, T.G. Santos, FSW of aluminium AA554 to steel DX54 with innovative overlap joint, Weld. World 61 (2017) 257e268.

[23] C. Zhang, Y. Cao, G. Huang, Q. Zeng, Y. Zhu, X. Huang, N. Li, Q. Liu, Influence of tool rotational speed on local microstructure, mechanical and corrosion behavior of dissimilar AA2024/7075 joints fabricated by friction stir welding,
J. Manuf. Process. 49 (2020) 214e226.

[24] T. Wang, H. Sidhar, R.S. Mishra, Y. Hovanski, P. Upadhyay, B. Carlson, Effect of hook characteristics on the fracture behaviour of dissimilar friction stir wel- ded aluminium alloy and mild steel sheets, Sci. Technol. Weld. Join. 24 (2) (2019) 178e184.

[25] K. Chen, X. Liu, J. Ni, Effects of process parameters on friction stir spot welding of aluminum alloy to advanced high-strength steel, ASME J. Manuf. Sci. Eng. 139p (81016) (2017) 1e9.

[26] E. Fereiduni, M. Movahedi, A.H. Kokabi, H. Najafi, Effect of dwell time on joint interface microstructure and strength of dissimilar friction stir spot-welded Al-5083 and St-12 alloy sheets, Metal, Mater. Trans. A

48A (2017) 1744e1758.

[27] R. Heideman, C. Johnson, S. Kou, Metallurgical analysis of Al/Cu friction stir spot welding, Sci. Technol. Weld. Join. 15 (7) (2010) 597e604.

[28] N. Sharma, Z.A. Khan, A.N. Siddiquee, Friction stir welding of aluminum to copper-an overview, Trans. Nonferrous Met. Soc. China 27 (10) (2017) 2113e2136.

[29] S. Manickam, C. Rajendran, V. Balasubramanian, Investigation of FSSW pa- rameters on shear fracture load of AA6061 and copper alloy joints, Heliyon 6 (2020) e04077.

[30] U. Suhuddin, V. Fischer, F. Kroeff, J.F. dos Santos, Microstructure and me- chanical properties of friction spot welds of dissimilar AA5754 Al and AZ31 Mg Alloys, Mater. Sci. Eng., A 590 (2014) 384e389.

[31]

[32] V.P. Singh, S.K. Patel, A. Ranjan, B. Kuriachen, Recent research progress in solid state friction-stir welding of aluminiumemagnesium alloys: a critical review, J. Mater. Res. Technol. 9 (3) (2020) 6217e6256.

[33] S. Wu, T. Sun, Y. Shen, Y. Yan, R. Ni, W. Liu, Conventional and swing friction stir spot welding of aluminum alloy to magnesium alloy, Int. J. Adv. Manuf. Technol. 116 (2021) 2401e2412.

[34] I.J. Ibrahim, G.G. Yapici, Application of a novel friction stir spot welding pro- cess on dissimilar aluminum joints, J. Manuf. Process. 35 (2018) 282e288.

[35] M. Paidar, R.V. Vignesh, A. Khorram, O.O. Ojo, A. Rasaoulpouraghdam, I. Pustokhina, Dissimilar modified friction stir clinching of 2024-6061 aluminum alloys: effects of materials positioning, J. Mater. Res. Technol. 9 (3) (2020) 6037e6047.

[36] V.A. Karkhin, Thermal Processes in Welding, Springer Nature Singapore Pte, Singapore, 2019.

[37] D. Radaj, Heat Effects of Welding: Temperature Field,

Residual Stress, Distortion, first ed., Springer-Verlag, Berlin, 1992.

[38] J.F. Lancaster, Metallurgy of Welding, sixth ed., Abington Publishing, Cam- bridge, 1999.

[39] Z. Zhang, B.L. Xiao, D. Wang, Z.Y. Ma, Effect of Alclad layer on material flow and defect formation in friction-stir-welded 2024 aluminum alloy, Metall. Mater. Trans. A 42A (2011) 1717e1726.

[40] S.R. Yazdi, B. Beidokhti, M. Haddad-Sabzevar, Pinless tool for FSSW of AA6061- T6 aluminum alloy, J. Mater. Process. Technol. 267 (2019) 44e51.

[41] O. Zareie, S.M. Mousavizade, H.R. Ezatpour, H. Zareie, N. Farmanbar, Effect of plunging depth and dwelling time on microstructure and mechanical prop- erties of 6061 aluminum alloy welded by protrusion friction stir spot welding, Weld. World 64 (2020) 785e805.

[42] Y. Gao, Y. Liang, X. Ren, M. Paidar, Pre-hole friction stir spot welding (PFSSW) for dissimilar welding of AA2219 to AA3003, Vacuum 182 (2020) 109688:1e7.

[43] W. Wang, T. Li, K. Wang, J. Cai, K. Qiao, Effect of travel speed on the stress corrosion behavior of friction stir welded 2024-T4 aluminum alloy, J. Mater. Eng. Perform. 25 (5) (2016) 1820e1828.

[44] I.J. Polmear, Light Alloys, third ed., Arnold, London, 1995.

[45] B. Bagheri, M. Abbasi, M. Givi, Effects of vibration on microstructure and thermal properties of friction stir spot welded (FSSW) aluminum alloy (Al5083), Int. J. Precis. Eng. Manuf. 20 (2019) 1219e1227.

[46] G.E. Dieter, Mechanical Metallurgy, McGraw-Hill Book Company (UK) Ltd, London, 1988.

[47] S. Horie, K. Shinozaki, M. Yamamoto, T.H. North, Experimental investigation of material flow during friction stir spot welding, Sci. Technol. Weld. Join. 15 (8) (2010) 666e670.

[48] M. de Leon, H.-S. Shin, Material flow behaviours during friction stir spot welding of lightweight alloys using pin and

pinless tools, Sci. Technol. Weld. Join. 21 (2) (2016) 140e146.

[49] A. Hirose, H. Todaka, H. Yamaoka, N. Kurosawa, K.F. Kobayashi, Quantitative evaluation of softened regions in weld heat-affected zones of 6061-T6 aluminum alloy-characterizing of the laser beam welding process, Metall. Mater. Trans. A 30 (1999) 2115e2120.

[50] N. Pathak, K. Bandyopadhyay, M. Sarangi, S.K. Panda, Microstructure and mechanical performance of friction stir spot-welded aluminum-5754 sheets, J. Mater. Eng. Perform. 22 (2013) 131e144.

[51] Y. Guishen, C. Xin, W. Zitao, Mechanical performance optimization and microstructure analysis of similar thin AA6061-T6 sheets produced by swept friction stir spot welding, Int. J. Adv. Manuf. Technol. 118 (2022) 1829e1841.